

Hofstadter spectrum in electric and magnetic fields.

Alejandro Kunold¹, Manuel Torres²

¹Departamento de Ciencias Básicas,
Universidad Autónoma Metropolitana-Azcapotzalco,
Av. San Pablo 180, México D. F. 02200, México,
Email:akb@correo.azc.uam.mx

²Instituto de Física,
Universidad Nacional Autónoma de México,
Apartado Postal 20-364, México D.F. 01000, México,
Email:torres@fisica.unam.mx

February 2, 2008

Abstract

The problem of Bloch electrons in two dimensions subject to magnetic and intense electric fields is investigated. Magnetic translations, electric evolution and energy translation operators are used to specify the solutions of the Schrödinger equation. For rational values of the magnetic flux quanta per unit cell and commensurate orientations of the electric field relative to the original lattice, an extended superlattice can be defined and a complete set of mutually commuting space-time symmetry operators is obtained. Dynamics of the system is governed by a finite difference equation that exactly includes the effects of: an arbitrary periodic potential, an electric field orientated in a commensurable direction of the lattice, and coupling between Landau levels. A weak periodic potential broadens each Landau level in a series of minibands, separated by the corresponding minigaps. The addition of the electric field induces a series of avoided and exact crossing of the quasienergies, for sufficiently strong electric field the

spectrum evolves into equally spaced discrete levels, in this “magnetic Stark ladder” the energy separation is an integer multiple of $\hbar E/aB$, with a the lattice parameter.

1 Introduction

The problem of electrons moving under the simultaneous influence of a periodic potential and a magnetic field has been discussed by many authors [1, 2, 3, 4, 5, 6, 7, 8]; the spectrum displays an amazing complexity including various kinds of scaling and a Cantor set structure [9]. Some of these results had been used in order to disclose the topological structure of the Hall conductance within the linear response theory [10, 11, 12]. The addition of an electric field leads to interesting new phenomena that makes its analysis worthwhile. For example, it has been suggested that as the strength of the electric field increases the longitudinal quasi-momentum is quantized leading to the appearance of a “magnetic Stark ladder”, in which the bands are replaced by a series of quasi discrete levels [13]. The quantization of the spectrum also affects the localization properties of electron wave packets [14, 15].

We consider the problem of an electron moving in a two-dimensional lattice in the presence of applied magnetic and electric fields. We refer to this as the electric-magnetic Bloch problem (EMB). The corresponding magnetic Bloch system (MB) has a long and rich history. An early important contribution was made by Peierls [1] who suggested the substitution of the Bloch index \mathbf{k} by the operator $(\mathbf{p} - e\mathbf{A})$ in the $B = 0$ dispersion relation $\epsilon(\mathbf{k})$, which is then treated as an effective single-band Hamiltonian. The symmetries of the MB problem were analyzed by Zak [3, 6, 8], who worked out the representation theory of the magnetic-translations group. The renowned Harper equation was derived assuming a tight-binding approximation in which the magnetic field acts as a perturbation that splits the Bloch bands [2]. Rauh derived a dual Harper equation in the opposite limit of intense magnetic field [5], here the periodic potential acts as a perturbation that broadens the Landau levels, in this case the Harper equation takes the form

$$c_{m-1} + 2 \cos(2\pi\sigma m + \kappa) c_m + c_{m+1} = \varepsilon c_m. \quad (1)$$

where $\sigma = 1/\phi$ is the inverse of magnetic flux ϕ in a cell in units of \hbar/e . The studies of the butterfly spectrum by Hofstadter and others have since

created an unceasing interest in the problem because of the beautiful self-similar structure of the butterfly spectrum [9, 16]. Remarkably, an experimental realization of the Hofstadter butterfly was achieved considering the transmission of microwaves [17] and acoustic waves [18] through an array of scatterers. However, the study of these phenomena in electronic transport has only recently become experimentally accessible with the developments in the fabrication of antidot arrays in lateral superlattices by ion beam and atomic force lithography [19, 20]. For example, a signal of the Hofstadter Butterfly spectrum through the measurement of the magnetoresistance and Hall conductance in artificial arrays of anti quantum dots has just been reported [21]. It is also worthwhile to point out that Aubry and Andre [22] utilized Eq. 1 to model a one dimensional system that develops a metal-insulator transition; this transition, arises from the competing effects of two potentials terms, which are periodic but incommensurate with one another.

The symmetries of the EMB problem were analyzed by Ashby and Miller, who constructed the group of the electric-magnetic translation operators, and worked out their irreducible representations [23]. The properties of the electric-magnetic operators were utilized in order to derive a finite difference equation that governs the dynamics of the EMB problem when the coupling between Landau levels can be neglected [13]. In this paper we shall derive the equation that applies under most general conditions. Magnetic translations, electric evolution and energy translation operators are used to specify the solutions of the Schrödinger equation, commensurability conditions must be implemented in order to obtain a set of mutually commuting space-time symmetry operators. In addition to the broadening of the Landau levels produced by the periodic potential, the electric field induces a series of avoided and exact level crossing that yields a generalized Hofstadter spectrum, with an interesting pattern that arises out of the competition between by the lattice potential and the external \mathbf{E} and \mathbf{B} fields. For sufficiently strong electric field the spectrum evolves into equally spaced discrete levels, in this “magnetic Stark ladder” the energy separation is an integer multiple of $\hbar E/aB$, with a the lattice parameter.

The paper is organized as follows. In the next section we present the model that describes the EMB problem and construct its symmetry operators. In Section 3 we describe the commensurability conditions required to have simultaneously commuting operators, they are exploited in order to construct an appropriated wave function basis. We derive an effective equation (30), in which the “evolution” is determined by a differential equation with

respect to the longitudinal pseudomomentum. The derivation of the finite difference equation that governs the dynamics of the system is presented in Section 4. Results for the energy spectrum are presented, and are also discussed from the perspective of the adiabatic approximation. The last section contains a summary of our main results.

2 The electric-magnetic Bloch problem

2.1 The model

Let us consider the motion of an electron in a two-dimensional periodic potential V , subject to a uniform magnetic field B perpendicular to the plane and to a constant electric field \mathbf{E} , lying on the plane according to $\mathbf{E} = E(\cos \theta, \sin \theta)$ with θ the angle between \mathbf{E} and the lattice x -axis. The dynamics of the electron is governed by a time-dependent Schrödinger equation that for convenience is written as

$$S|\psi\rangle = \left[\frac{1}{2m^*} (\Pi_x^2 + \Pi_y^2) + V - \Pi_0 \right] |\psi\rangle = 0, \quad (2)$$

here m^* is the effective electron mass, $\Pi_\mu = p_\mu + eA_\mu$, with $p_\mu = (i\hbar\partial/\partial t, -i\hbar\nabla)$. Throughout the paper energy and lengths are measured in units of $\hbar\omega_c = \frac{\hbar eB}{m^*}$, and $\ell_0 = \sqrt{\frac{\hbar}{eB}}$, respectively, where ω_c is the cyclotron frequency and ℓ_0 the magnetic length. So, unless specified, we set $\hbar = e = m^* = 1$; although B can also be omitted from the expressions, we find convenient to explicitly display it. Covariant notation will be used to simplify the expressions, *e.g.* $x_\mu = (t, \mathbf{x}) = (t, x, y)$.

Equation (2) can be considered as an eigenvalue equation for the operator S with eigenvalue 0. The gauge potential is written in an arbitrary gauge, it includes two gauge parameters α , and β , the final physical results should be of course, independent of the gauge. Hence the components of the gauge

potentials are written as

$$\begin{aligned} A_0 &= \left(\beta - \frac{1}{2}\right) \mathbf{x} \cdot \mathbf{E}, \\ A_x &= -\left(\beta + \frac{1}{2}\right) E_x t + \left(\alpha - \frac{1}{2}\right) B y, \\ A_y &= -\left(\beta + \frac{1}{2}\right) E_y t + \left(\alpha + \frac{1}{2}\right) B x. \end{aligned} \tag{3}$$

The symmetrical gauge is recovered for $\alpha = 0$, whereas the Landau gauge corresponds to the selection $\alpha = 1/2$. If $\beta = 1/2$ all the electric field contribution appears in the vector potential, instead if $\beta = -1/2$ it lies in the scalar potential and the Schrödinger equation becomes time independent, however even in this case a time dependence will slip into the problem through the symmetry operators. A general two-dimensional periodic potential can be represented in terms of its Fourier decomposition

$$V(x, y) = \sum_{r,s} v_{rs} \exp\left(i\frac{2\pi r x}{a} + i\frac{2\pi s y}{a}\right). \tag{4}$$

For specific numerical results we shall use the potential

$$V(x, y) = U_0 \left[\cos\left(\frac{2\pi x}{a}\right) + \lambda \cos\left(\frac{2\pi y}{a}\right) \right]. \tag{5}$$

λ is a parameter that can be varied in order to have an anisotropic lattice; $\lambda = 1$ corresponds to the isotropic limit.

2.2 Electric evolution and magnetic translations

Let $(t, \mathbf{x}) \rightarrow (t + \tau, \mathbf{x} + \mathbf{R})$ be a uniform translation in space and time, where τ is an arbitrary time and \mathbf{R} is a lattice vector. The classical equations of motion remain invariant under these transformations; whereas the Schrödinger equation does not, the reason being the space and time dependence of the gauge potentials. Nevertheless, quantum dynamics of the system remain invariant under the combined action of space-time translations and gauge transformations. The electric and magnetic translation operators are defined as

$$T_0(\tau) = \exp(-i\tau\mathcal{O}_0), \quad T_j(a) = \exp(ia\mathcal{O}_j), \tag{6}$$

with $j = x, y$ and the electric-magnetic symmetry generators are written as covariant derivatives $\mathcal{O}_\mu = p_\mu + \Lambda_\mu$, with the components of the dual gauge potentials Λ_μ given by

$$\begin{aligned}\Lambda_0 &= A_0 + \mathbf{x} \cdot \mathbf{E}, \\ \Lambda_x &= A_x + By + E_xt, \quad \Lambda_y = A_y - Bx + E_yt.\end{aligned}\tag{7}$$

It is straightforward to prove that the operators in (6) are indeed symmetries of the Schrödinger equation; they commute with the operator S in Eq. (2). Similar expressions for the electric-magnetic operators were given by Ashby and Miller [23], however their definition included simultaneous space and time translations; we deemed it more convenient to separate the effect of the time evolution generated by the T_0 to that of the space translations generated by T_j . The following commutators can be worked out

$$\begin{aligned}[\Pi_0, \Pi_j] &= -iE_j, & [\Pi_1, \Pi_2] &= -iB, \\ [\mathcal{O}_0, \mathcal{O}_j] &= iE_j, & [\mathcal{O}_1, \mathcal{O}_2] &= iB, \\ [\Pi_\mu, \mathcal{O}_\nu] &= 0.\end{aligned}\tag{8}$$

Notice that the electric-magnetic generators \mathcal{O}_μ have been defined in such a form that they commute with all the velocity operators Π_ν . The Schrödinger equation and the symmetry operators are expressed in terms of covariant derivatives Π_μ and \mathcal{O}_μ , respectively. A dual situation in which the roles of Π_μ and \mathcal{O}_μ are interchanged can be considered. The dual problem corresponds to a simultaneous reverse in the directions of B and \mathbf{E} . We notice that the commutators in the second line of Eq. (8) are part of the Lie algebra of the EM-Galilean two dimensional group [24, 25]. This group is obtained when the usual rotation and boost operators of the planar-Galilean group are replaced by their electric-magnetic generalization in which the operators are enlarged by the effect of a gauge transformation.

3 Electric-magnetic Bloch Functions

3.1 Commensurability conditions

In order to construct a complete base that expands the wave function we require the symmetry operators to commute with each other. However we

have

$$T_\mu T_\nu = e^{-c^\mu c^\nu [\mathcal{O}_\mu, \mathcal{O}_\nu]} T_\nu T_\mu, \quad (9)$$

where $c^0 = -\tau$, and $c^1 = c^2 = a$. A set of simultaneously commuting symmetry operator can be found if appropriated commensurate conditions are imposed, we follow a three step method to find them:

1. First we consider a frame rotated at angle θ , with axis along the longitudinal and transverse direction relative to the electric field. An orthonormal basis for this frame is given by $\mathbf{e}_L = (\cos\theta, \sin\theta)$, $\mathbf{e}_T = (-\sin\theta, \cos\theta)$ and $\mathbf{e}_3 = \mathbf{e}_L \times \mathbf{e}_T$. The electric field is parallel to \mathbf{e}_L and the magnetic field points along \mathbf{e}_3 . We assume a particular orientation of the electric field, for which the following condition holds

$$\tan\theta = \frac{E_y}{E_x} = \frac{m_2}{m_1}, \quad (10)$$

where m_1 and m_2 are relatively prime integers. This condition insures that spatial periodicity is also found both along the transverse and the longitudinal directions. Hence, we define a rotated lattice spanned by the longitudinal $\mathbf{b}_L = b\mathbf{e}_L$ and transverse $\mathbf{b}_T = b\mathbf{e}_T$ vectors, where $b = a\sqrt{m_1^2 + m_2^2}$. The spatial components of the symmetry generator \mathcal{O} are projected along the longitudinal and transverse directions: $\mathcal{O}_L = \mathbf{e}_L \cdot \mathcal{O}$ and $\mathcal{O}_T = \mathbf{e}_T \cdot \mathcal{O}$. It is readily verified that $[\mathcal{O}_L, \mathcal{O}_T] = 0$.

2. For the rotated lattice, we regard the number of flux quanta per unit cell to be a rational number p/q , that is

$$\phi \equiv \frac{1}{\sigma} = \frac{B b^2}{2\pi} = \frac{p}{q}. \quad (11)$$

We can then define a extended superlattice. A rectangle made of q adjacent lattice cells of side b contains an integer number of flux quanta. The basis vectors of the superlattice are chosen as $q\mathbf{b}_L$ and \mathbf{b}_T . Under these conditions the longitudinal and transverse magnetic translations $T_L(qb) = \exp(iqb\mathcal{O}_L)$ and $T_T(b) = \exp(ib\mathcal{O}_T)$ define commuting symmetries under displacements $q\mathbf{b}_L$ and \mathbf{b}_T . Henceforth we shall either use the subindex (L, T) or $(1, 2)$ to label the longitudinal and transverse directions.

3. We observe that T_0 and $T_L(qb)$ commute with T_T . Yet they fail to commute with each other:

$$T_0(\tau) T_L(qb) = e^{-iqb\tau E} T_L(qb) T_0(\tau). \quad (12)$$

However the operators T_0 and $T_L(qb)$ will commute with one another by restricting time, in the evolution operator, to discrete values with period

$$\tau = n\tau_0, \quad n \in \mathbb{Z}, \quad \tau_0 = \frac{2\pi}{qbE} = \frac{1}{p} \left(\frac{b}{v_D} \right), \quad (13)$$

where the drift velocity is $v_D = E/B$ and we utilized Eq. (11) to write the second equality. b/v_D is the period of time it takes an electron with drift velocity v_D to travel between lattice points. Eq. (13) can be interpreted as the condition that the ratio of two energy scales is an integer: as we shall see (σbE) is the magnetic-Stark ladder spacing, whereas $(2\pi v_D/b)$ is the quasienergy Brillouin width; hence Eq. (13) represents the ratio of these two quantities.

We henceforth consider that the three conditions (10), (11), and (13) hold simultaneously. In this case the three EM operators: the electric evolution $\mathcal{T}_0 \equiv T_0(\tau_0)$, and the magnetic translations $\mathcal{T}_L \equiv T_L(qb)$, and $\mathcal{T}_T \equiv T_T(b)$ form a set of mutually commuting symmetry operators. In addition to the symmetry operators it is convenient to define the energy translation operator [26]

$$\mathcal{T}_E = \exp \left(-i \frac{2\pi}{\tau_0} t \right), \quad (14)$$

that produces a finite translation in energy by $2\pi/\tau_0 \equiv qbE$. \mathcal{T}_E commutes with the three symmetry operators but not with S . Its eigenfunctions

$$\mathcal{T}_E \psi = e^{iqbE\vartheta} \psi, \quad (15)$$

define a quasitime ϑ modulo τ_0 .

3.2 Wave function and generalized Bloch conditions

Having defined \mathcal{T}_0 , \mathcal{T}_L and \mathcal{T}_T that commute with each other and also with S , it is possible to seek for solutions of the Schrödinger equation labeled by

the quasienergy (\mathcal{E}) and the longitudinal (k_1) and transverse (k_2) quasimomentum according to

$$\begin{aligned}\mathcal{T}_0 |\mathcal{E}, k_1, k_2\rangle &= e^{-i\tau_0 \mathcal{E}} |\mathcal{E}, k_1, k_2\rangle, \\ \mathcal{T}_L |\mathcal{E}, k_1, k_2\rangle &= e^{ik_1 qb} |\mathcal{E}, k_1, k_2\rangle, \\ \mathcal{T}_T |\mathcal{E}, k_1, k_2\rangle &= e^{ik_2 b} |\mathcal{E}, k_1, k_2\rangle.\end{aligned}\tag{16}$$

The magnetic Brillouin zone (MBZ) is defined by $k_1 \in [0, 2\pi/qb]$ and $k_2 \in [0, 2\pi/b]$. Similarly the quasienergy \mathcal{E} is defined modulo $2\pi/\tau_0 = qbE$. If a restricted energy scheme is selected for the energy, the first energy Brillouin region is defined by the condition $\mathcal{E} \in [0, 2\pi/\tau_0]$. We shall find convenient to perform a canonical transformation to new variables according to

$$\begin{aligned}Q_0 &= t, & P_0 &= \mathcal{O}_0 - \frac{1}{2}E^2, \\ Q_1 &= \Pi_2 + E, & P_1 &= \Pi_1, \\ Q_2 &= \mathcal{O}_1 - Et, & P_2 &= \mathcal{O}_2 + E,\end{aligned}\tag{17}$$

that satisfy the commutation rules $[Q_\mu, P_\nu] = -ig_{\mu\nu}$, $g_{\mu\nu} = \text{Diag}(-1, 1, 1)$. Applied to Eq. (2) the transformation yields for the Schrödinger equation

$$P_0 |\psi\rangle = H |\psi\rangle, \quad H = \left[\frac{1}{2} (P_1^2 + Q_1^2) + V(x, y) - EP_2 \right]. \tag{18}$$

In this equation (x, y) must be expressed in terms of the new variables:

$$\begin{aligned}\frac{x}{a} &= \frac{m_1}{b} (Q_1 - P_2) - \frac{m_2}{b} (Q_2 - P_1), \\ \frac{y}{a} &= \frac{m_2}{b} (Q_1 - P_2) + \frac{m_1}{b} (Q_2 - P_1).\end{aligned}\tag{19}$$

On the other hand, the EM-symmetry operators and the energy translation operator take the form:

$$\begin{aligned}\mathcal{T}_0 &= e^{-i\tau_0 P_0}, & \mathcal{T}_L &= e^{iqb(Q_2 + EP_0)}, \\ \mathcal{T}_T &= e^{ibP_2}, & \mathcal{T}_E &= e^{-i\frac{2\pi}{\tau_0} Q_0}.\end{aligned}\tag{20}$$

Notice that these operators do not depend on the variables P_1, Q_1 . Thus, it is natural to split the phase space (Q_μ, P_μ) in the (Q_1, P_1) and the $(Q_0, P_0; Q_2, P_2)$ variables. For the first set a harmonic oscillator base is used. Whereas for

the subspace generated by the variables $(Q_0, P_0; Q_2, P_2)$, we observe that the operators $(\mathcal{T}_0^i, \mathcal{T}_L^j, \mathcal{T}_T^k, \mathcal{T}_E^l)$ with all possible integer values of (i, j, k, l) form a complete set of operators. The demonstration follows similar steps as those presented by Zak in reference [27]. Hence a complete set of functions, for the subspace $(Q_0, P_0; Q_2, P_2)$, is provided by the eigenfunctions of the operators $(\mathcal{T}_0^i, \mathcal{T}_L^j, \mathcal{T}_T^k, \mathcal{T}_E^l)$. As starting point, we select a base of eigenvalues of the following operators

$$\begin{aligned} A^\dagger A |\mu, \mathcal{E}, k_2\rangle &= \mu |\mu, \mathcal{E}, k_2\rangle, \\ P_0 |\mu, \mathcal{E}, k_2\rangle &= \mathcal{E} |\mu, \mathcal{E}, k_2\rangle, \\ P_2 |\mu, \mathcal{E}, k_2\rangle &= k_2 |\mu, \mathcal{E}, k_2\rangle, \end{aligned} \tag{21}$$

where A and A^\dagger are the lowering and raising operators of the μ -Landau level:

$$A = \frac{1}{\sqrt{2}}(P_1 - iQ_1), \quad A^\dagger = \frac{1}{\sqrt{2}}(P_1 + iQ_1). \tag{22}$$

It is straightforward to verify that these states fulfill the required eigenfunction condition (16) for the \mathcal{T}_0 and \mathcal{T}_T operators. On the other hand \mathcal{T}_L induces a shift in the \mathcal{E} and k_2 labels, while \mathcal{T}_E induces a shift qbE in the \mathcal{E} label. The previous considerations suggest that a state $|\vartheta, \mathcal{E}, k_1, k_2\rangle$ that is a simultaneous eigenfunction of the four operators $\mathcal{T}_E, \mathcal{T}_0, \mathcal{T}_L$ and \mathcal{T}_T with the required eigenvalues (Eqs. 15 and 16), can be constructed as a linear superposition of states of the form $[\mathcal{T}_L]^l [\mathcal{T}_L \mathcal{T}_E^{-1}]^m |\mu, \mathcal{E}, k_2\rangle$. We write down the state, and verify their correctness:

$$|\vartheta, \mathcal{E}, k_1, k_2\rangle = \sum_l [\mathcal{T}_L e^{-iqbk_1}]^l \sum_{\mu, m} c_m^\mu [e^{i\sigma b Q_2} e^{i\sigma b (E\vartheta - k_1)}]^m |\mu, \mathcal{E}, k_2\rangle. \tag{23}$$

It is easy to check that this function satisfies the three eigenvalue equations for the symmetry operators in (16). Additionally it can be verified that the eigenvalue condition (15) for the energy translation operator is also fulfilled by imposing the periodicity condition $c_{m+p}^\mu = c_m^\mu$. Every state in (23) yields a set of different eigenvalues, a condition that follows from the fact that the selected set of operators is complete, hence the base of eigenvalues in (23) is complete and orthonormal.

Up to this point we have constructed a base for the set of four $(\mathcal{T}_0, \mathcal{T}_L, \mathcal{T}_T, \mathcal{T}_E)$ operators, however the operator \mathcal{T}_E is not a symmetry of the problem,

consequently the solution of the Schrödinger is constructed as a superposition of all the states characterized by ϑ ; the state becomes

$$|\mathcal{E}, k_1, k_2\rangle = \int d\vartheta C(\vartheta) |\vartheta, \mathcal{E}, k_1, k_2\rangle = \sum_l [\mathcal{T}_L e^{-iqbk_1}]^l \sum_{\mu, m} b_m^\mu e^{i\sigma b(Q_2 - k_1)m} |\mu, \mathcal{E}, k_2\rangle, \quad (24)$$

where

$$b_m^\mu = \int d\vartheta C(\vartheta) c_m^\mu e^{iqbE\vartheta m}. \quad (25)$$

Equation (24) represents the correct state that satisfies the eigenvalue equations (16). It is convenient to recast it in a compact form as

$$|\mathcal{E}, \mathbf{k}\rangle = \mathcal{W}(k_1) |\mathcal{E}, k_2\rangle, \quad (26)$$

where $|\mathcal{E}, \mathbf{k}\rangle = |\mathcal{E}, k_1, k_2\rangle$, and the operator $\mathcal{W}(k_1)$ is defined as

$$\mathcal{W}(k_1) = \sum_l [\mathcal{T}_L e^{-iqbk_1}]^l = \sum_l e^{iqbl(EQ_0 + Q_2 - k_1)}. \quad (27)$$

whereas the ket $|\mathcal{E}, k_2\rangle$ is given by

$$|\mathcal{E}, k_2\rangle = \sum_{\mu, m} e^{i\sigma bm(Q_2 - k_1)} b_m^\mu |\mu, \mathcal{E}, k_2\rangle. \quad (28)$$

The previous expression stresses the fact that the quantity $e^{-i\sigma bm k_1} b_m^\mu$ does not depends on k_1 , this will be demonstrated below Eq. (45). These results will prove to be very useful to analyze the EM problem, in particular they allow us to obtain an effective Schrödinger equation where the “dynamics” is governed by the derivative with respect to the longitudinal pseudomomentum. Utilizing Eqs. (26) y (27) it is straightforward to prove the following relation

$$P_0 |\mathcal{E}, k_1, k_2\rangle = [P_0, \mathcal{W}] |\mathcal{E}, k_2\rangle + \mathcal{W} P_0 |\mathcal{E}, k_2\rangle = (\mathcal{E} - i\mathbf{E} \cdot \nabla_{\mathbf{k}}) |\mathcal{E}, k_1, k_2\rangle. \quad (29)$$

Thus the Schrödinger (18) can be recast as

$$(\mathcal{E} - i\mathbf{E} \cdot \nabla_{\mathbf{k}}) |\mathcal{E}, k_1, k_2\rangle = H |\mathcal{E}, k_1, k_2\rangle. \quad (30)$$

As it will be lately discussed, this form of the Schrödinger equation becomes very useful to prove various properties of the system, in particular the adiabatic solution of the problem.

The wave function takes a simply form if we adopt the (P_0, P_1, P_2) representation. In this case $\Psi_{\mathbf{k}}(p) = \langle P_0, P_1, P_2 | \mathcal{E}, k_1, k_2 \rangle$ yields

$$\Psi_{\mathbf{k}}(P) = \sum_{\mu, l, m} b_m^\mu \phi_\mu(P_1) e^{i(2\pi/b)(m+pl)k_1} \delta(P_0 - \mathcal{E} - lqbE) \delta\left(P_2 - k_2 + \frac{2\pi}{b}(m+pl)\right), \quad (31)$$

where $\phi_\mu(P_1)$ is the harmonic oscillator function in the P_1 representation

$$\phi_\mu(P_1) = \langle P_1 | \mu \rangle = \frac{1}{\sqrt{\pi^{1/2} 2^\mu \mu!}} e^{-P_1^2/2} H_\mu(P_1), \quad (32)$$

and $H_\mu(P_1)$ is the Hermite polynomial.

On the other hand, it is sometimes useful to restore the space-time representation of the wave function. This problem provides a good example of the use of canonical transformations in quantum mechanics. Identifying the matrices that relate the (x_μ, p_μ) variables to (Q_μ, P_μ) , it is possible to apply the method of reference [28] in order to obtain the desired transformation. The final result for the wave function in the space-time representation yields

$$\Psi_{\mathbf{k}}(t, \mathbf{x}) = e^{i\mathbf{k} \cdot \mathbf{x} - i\mathcal{E}t} u_{\mathbf{k}}(t, \mathbf{x}), \quad (33)$$

where the modulation function $u(t, \mathbf{x})$ is given by

$$u_{\mathbf{k}}(t, \mathbf{x}) = \frac{1}{\sqrt{2\pi}} e^{-ix_1[(\alpha-1/2)x_2+k_1]} e^{i(\beta+1/2)Et x_1} \times \sum_{\mu, l, m} i^\mu b_m^\mu e^{-iqbElt} e^{i\sigma b(k_1-x_2)(m+pl)} \phi_\mu\left(x_1 - k_2 + 2\pi \frac{m+pl}{b}\right), \quad (34)$$

here ϕ_μ is the same harmonic oscillator function Eq. (32), but now evaluated in the *space* representation. It is worthwhile to notice, that whereas there is not explicit gauge dependence for the wave function in the P representation (Eq. (31)), the dependence on the gauge parameters α and β becomes explicit in the space-time representation (Eq. (34)).

Solution (33,34) includes a superposition of Landau-type solutions originated beneath the spatial and time periodicity. The spatial periodicity is simply related to the external potential V . Whereas time periodicity arises from the conditions imposed to the symmetry operators in order to produce commuting symmetries; as discussed in Eq. (13), the period is given by the time that takes an electron to drift between contiguous lattice points. Notice that Eqs. (33,34) follows from the Bloch and Floquet theorem. However in the electric-magnetic case the modulation functions $u(t, \mathbf{x})$ are not strictly periodic, instead they satisfy the generalized Bloch conditions

$$\begin{aligned} u(t + \tau_0, x_1, x_2) &= e^{i\tau_0\Lambda_0} u(t, x_1, x_2), \\ u(t, x_1 + qb, x_2) &= e^{-iqb\Lambda_1} u(t, x_1, x_2), \\ u(t, x_1, x_2 + b) &= e^{-ib\Lambda_2} u(t, x_1, x_2), \end{aligned} \quad (35)$$

the phases are determined by the dual-gauge potential that appears in the symmetry operators Eq. (7). It is straightforward to verify that $u_{\mathbf{k}}$ in Eq. (34) satisfies these conditions. The generalized Bloch conditions for the magnetic-Bloch problem have been previously discussed, our results in (35) reduces to those in reference [7], when $\mathbf{E} = 0$ and the gauge $\alpha = 1/2$ is selected. Our results in (35) have been extended in order to include the electric field effects, furthermore they apply for an arbitrary gauge. The correct normalization conditions for the modulation function are obtained as follows

$$\frac{(2\pi)^2}{qb^2} \int_{\text{MUC}} d^2x u^*(t, x) u(t, x) = 1, \quad (36)$$

where MUC represents the magnetic cell defined by: $x_1 \in [0, qb]$ and $x_2 \in [0, b]$.

The function u satisfies conditions similar to those in Eq. (35) but in the MBZ. The MBZ is actually a torus T^2 , so the edges $(k_1 = 0, k_2)$ and $(k_1 = 2\pi/qb, k_2)$ must be identified as the same set of points, the wave function can differ at most by a total phase factor (similarly for the edges $(k_1, k_2 = 0)$ and $(k_1, k_2 = 2\pi/b)$):

$$u(k_1 + 2\pi/qb, k_2) = e^{if_1} u(k_1, k_2), \quad u(k_1, k_2 + 2\pi/b) = e^{if_2} u(k_1, k_2), \quad (37)$$

the functions $f_1(\mathbf{k})$ and $f_2(\mathbf{k})$ can be related with the quantized values of the Hall conductance [12], however instead of Eq. (35), these functions are not analytically known and must be computed numerically.

4 Harper generalized equation

4.1 Finite difference equation

The coefficient b_m^μ in Eq. (24) satisfies a recurrence relation that is obtained when this base is used to calculate the matrix elements of the Schrödinger equation (18). First, let us consider the contribution arising from the periodic potential in Eq. (4). The x and y coordinates are written in terms of the new variables (Q_1, P_1, Q_2, P_2) by means of Eq. (19), producing a term of the form $\exp[(i2\pi r m_1(Q_1 - P_2)/b)]$, and another contribution in which Q_1 and P_2 are replaced by Q_2 and P_1 . Once that Q_1 and P_1 are replaced by the raising and lowering operators in Eq. (22), one is lead to evaluate the matrix elements of the operator $D = \exp(zA^\dagger - z^*A)$ that generates coherent Landau states. A calculation yields

$$D^{\nu\mu}(z) = \langle \nu | \exp(zA^\dagger - z^*A) | \mu \rangle = e^{-\frac{1}{2}|z|^2} \begin{cases} (-z^*)^{\mu-\nu} \sqrt{\frac{\nu!}{\mu!}} L_\nu^{\mu-\nu}(|z|^2), & \mu > \nu, \\ z^{\nu-\mu} \sqrt{\frac{\mu!}{\nu!}} L_\mu^{\nu-\mu}(|z|^2), & \mu < \nu, \end{cases} \quad (38)$$

where L_μ^μ are the generalized Laguerre polynomial. The evaluation of the terms that include the P_2 operator is direct, because the base is a eigenvalue of this operator, on the other hand the operator $\exp[(i2\pi r m_1 Q_2)/b]$ acts as a translation operator that produces a shift on the index m of the b_m^μ coefficient. Taking into account these results, it is possible to demonstrate after a lengthly calculation that the Schrödinger equation (18) becomes

$$\sum_{t=-N}^{t=N} \mathbb{A}_m^t(k_1, k_2) \tilde{b}_{m+t} = (\mathcal{E} + Ek_2 + \sigma bEm) \tilde{b}_m. \quad (39)$$

Besides its dependence on the index m , \tilde{b}_m is a vector with L components and $\mathbb{A}_m^t(k_1, k_2)$ is a $L \times L$ matrix in the Landau space, according to

$$\begin{aligned} \tilde{b}_m &= \{b_m^\mu\} = (b_m^0, b_m^1, \dots, b_m^L), \\ (\mathbb{A}_m^t)^{\mu\nu} &= e^{-i\sigma b k_1 t} \sum_{r,s} B_m^{\mu\nu}(r, s) \delta_{t, rm_2 - sm_1}. \end{aligned} \quad (40)$$

In the previous expressions L is the highest Landau level included in the calculations, $N = \max\{(r, s)(m_1 + m_2)\}$ is related to the largest harmonic

in the Fourier decomposition of the periodic potential (4), and $B_m^{\nu\mu}(r, s)$ is given by

$$B_m^{\nu\mu}(r, s) = \begin{cases} (v_{00} + \mu + \frac{1}{2}) \delta^{\mu\nu}, & r, s = 0, \\ v_{rs} D^{\nu\mu}(H_{rs}) e^{iK_{rs}} e^{iM_{rs}[\sigma b(rm_2 - sm_1 + m) + k_2]} & r, s \neq 0, \end{cases} \quad (41)$$

the following definitions were introduced in the previous equation

$$\begin{aligned} H_{rs} &= \frac{\sqrt{2}\pi}{b} (m_2 - im_1)(ir + s), \\ K_{rs} &= \frac{2\pi^2}{b^2} (rm_2 - sm_1)(rm_1 + sm_2), \\ M_{rs} &= -\frac{2\pi}{b} (rm_1 + sm_2). \end{aligned} \quad (42)$$

We recall that the indexes (r, l) refer to the Fourier expansion of the periodic potential Eq. (4), whereas (m_1, m_2) correspond to the integers that determined the electric field orientation in Eq. (10).

Equation (39) describes the system in terms of a recurrence relation on a two dimensional (μ, m) basis. The coupling in m ranges from $m - N$ to $m + N$. We follow the method of reference [29] to recast the recurrence relation on m with N nearest-neighbor coupling into a tridiagonal vector recurrence relation. This is enforced by defining a N component vector

$$\tilde{c}_m = (\tilde{b}_{Nm-1}, \tilde{b}_{Nm}, \tilde{b}_{Nm+1}, \dots, \tilde{b}_{N(m+1)-1}) , \quad (43)$$

and matrices Q_m^\pm and Q_m with elements

$$\begin{aligned} Q_m^-(k_1, k_2) &= \begin{pmatrix} \mathbb{A}_{Nm}^{-N} & \mathbb{A}_{Nm}^{-N+1} & \dots & \mathbb{A}_{Nm}^{-1} \\ 0 & \mathbb{A}_{Nm+1}^{-N} & \dots & \mathbb{A}_{Nm+1}^{-2} \\ \vdots & \vdots & \ddots & \vdots \\ 0 & 0 & \dots & \mathbb{A}_{N(m+1)-1}^{-N} \end{pmatrix}, \\ Q_m(k_1, k_2) &= \begin{pmatrix} \mathbb{A}_{Nm}^0 & \mathbb{A}_{Nm}^1 & \dots & \mathbb{A}_{Nm}^{N-1} \\ \mathbb{A}_{Nm+1}^{-1} & \mathbb{A}_{Nm+1}^0 & \dots & \mathbb{A}_{Nm+1}^{N-2} \\ \vdots & \vdots & \ddots & \vdots \\ \mathbb{A}_{N(m+1)-1}^{1-N} & \mathbb{A}_{N(m+1)-1}^{2-N} & \dots & \mathbb{A}_{N(m+1)-1}^0 \end{pmatrix}. \end{aligned} \quad (44)$$

Using the fact that $Q_m^+ = (Q_m^-)^\dagger$, Eq. (39) can be reorganized as a tridiagonal recurrence relation

$$Q_m^- \tilde{c}_{m-1} + Q_m \tilde{c}_m + Q_m^+ \tilde{c}_{m+1} = [(\mathcal{E} + Ek_2 + \sigma bEm) I_N + \sigma bED_N] \tilde{c}_m. \quad (45)$$

Here, \tilde{c}_m is N -dimensional vector according to the definition (43), additionally each one of its components is a L dimensional vector due to its dependence on the Landau index Eq. (40). I_N is the unit matrix and $D_N = \text{Diag}(0, 1, 2, \dots, N-1)$. Likewise, each of the components of the matrices Q_m , I_N , and D_N are $L \times L$ matrices relative to the Landau contributions. In relation with Eq. (28) it was mentioned that the quantity $e^{-i\sigma b k_1} \tilde{c}_m$ does not explicitly depend on the longitudinal pseudomomentum component k_1 , this can be easily verified if the substitution $\tilde{c}'_m = e^{-i\sigma b k_1} \tilde{c}_m$ is incorporated into Eq. (45), then using Eqs. (40) and (44), it is straightforward to verify that \tilde{c}'_m is indeed independent of k_1 .

Eq. (45) is one of our main results, and deserves to be emphasized. It is a generalization of the Harper equation that exactly includes the following effects: (1) an arbitrary periodic potential, (2) an electric field orientated in a commensurable direction of the lattice, and (3) the coupling between different Landau levels. So far, no approximations are involved, consequently it holds under most general conditions. In practice, only a finite number L of Landau levels can be included on the calculations, but a very good convergence can be obtained with a reasonable small selection for L . Previous known results are recovered if some approximations are enforced: (i) if the electric field is switched off, its orientation is meaningless, so the integers (m_1, m_2) can be set to $m_1 = 1$ and $m_2 = 0$, in this case Eq. (45) reduces to the model previously discussed by Petschel and Geisel [30]. (ii) If $\mathbf{E} = 0$ and additionally the coupling between different Landau bands is neglected and the potential is taken as the sum of cosines given in Eq. (5), then the system reduces to a set of Harper equations (1), one for each Landau band.

Let us return to the case that includes the electric field. Equation (45) describes the system dynamics under most general conditions; in spite of its complicated structure the equation can be solved by the matrix continued fraction methods. However, a considerable simplification is obtained if the electric field is aligned along the x -lattice axis, i.e. $(m_1 = 1, m_2 = 0)$. Henceforth, we consider that the electric field is orientated along the x -axis $(m_1 = 1, m_2 = 0)$, so $b \equiv a$ and additionally that the periodic potential takes the form given in (5). The dimension N of the vectors \tilde{c}_m and matrices in

Eqs. (43) and (44) reduces to $N = \max\{(r, s)(m_1 + m_2)\} = 1$, hence the dimensions of $\tilde{c}_m \equiv c_m$ and Q reduce to include only the Landau indexes. Using equations (40), (41) and (44) the matrices Q become

$$\begin{aligned} (Q_m^+)^{\mu\nu} &\equiv (Q^+)^{\mu\nu} = \frac{\lambda\pi K}{2(1+\lambda)a^2} e^{i\sigma b k_1} D^{\mu\nu}(\sqrt{\pi\sigma}), \\ (Q_m)^{\mu\nu} &= \frac{\pi K}{2(1+\lambda)a^2} e^{i(2\pi\sigma m + \sigma b k_2)} D^{\mu\nu}(\sqrt{\pi\sigma}) + c.c., \end{aligned} \quad (46)$$

here the parameter K is a measure of the strength of the coupling between Landau bands

$$K = \frac{ma^2 U_0 (1 + \lambda)}{\hbar^2 \pi}. \quad (47)$$

Taking into account these simplifications and that D_N cancels out, we find that Eq. (45) reduces to

$$Q^- c_{m-1} + Q_m c_m + Q^+ c_{m+1} = (\mathcal{E} + Ek_2 + \sigma b Em) c_m. \quad (48)$$

4.2 Numerical results

The generalized Harper equation is given by a tridiagonal infinite recurrence relation (48). If \mathbf{E} is switched off, the equation becomes periodic with period p , in this case the equation can be recast as a finite $pL \times pL$ matrix that can be solved by a direct diagonalization. However, the introduction of \mathbf{E} breaks the periodicity, and most of the methods used to solve the Harper equation break down. Eq. (48) was solved using an expansion of the associated Green's function into matrix continued fractions (MCFs) [29]. The energy spectrum is determined detecting the change of sign in the Green's functions that appear in the vicinity of a pole. The density of states can be obtained from the expression

$$N(\mathcal{E}) = \frac{i}{\pi} \text{Tr } \tilde{G}(\mathcal{E}) = \mp \frac{1}{\pi} \text{Im} [\text{Tr } G^\pm(\mathcal{E})], \quad (49)$$

where the discontinuity in Green's function is given by $\tilde{G}(\mathcal{E}) = G^+(\mathcal{E}) - G^-(\mathcal{E})$, and the retarded and advanced Green's functions are defined on the side limits $G^\pm(\mathcal{E}) = \lim_{\epsilon \rightarrow 0} G(\mathcal{E} \pm i\epsilon)$. The numerical solution is obtained by truncating the iteration of the (MCFs) after the M -th term. The solution

converges if M is large enough, in the calculations we observe that in order to obtain a convergence with a precision of one part in 10^7 , the cutoff can be selected as $M \approx 100$.

In our calculations we have used the effective mass $m^* = 0.067m_e$ typical for electrons in *GaAs* and a superlattice constant $a = 100 \text{ nm}$ [21]. The rescaled energy spectrum $\mathcal{E}/[U_0 e^{-\pi\sigma/2}]$ is shown in Fig. 1 for the lowest Landau level, a weak modulation is considered ($U_0 = 0.5 \text{ meV}$) so the $\mu - \nu$ Landau mixing is negligible. The electric field intensity is $E = 0.5 \text{ V/cm}$ corresponding to a ratio of the electric to the periodic potential of $\rho = eaE/U_0 = 0.02$. In the strong magnetic region, $\sigma \in [0, 1]$, the Hofstadter butterfly is clearly depicted. A distorted replica of the butterfly spectrum can be still observed in the region $\sigma \in [1, 2]$. As the magnetic field loses intensity, the effect of the electric field becomes dominant, the butterfly is replaced by discrete levels separated in regular intervals, i.e. a Stark ladder. Although, $\rho = eaE/U_0$ is small, there is a regime in which the electric field dominates over the lattice potential contribution, we can trace down the origin of this effect to Eqs. (38) and (46) showing that the periodic contribution is modulated by a factor $e^{-\pi\sigma/2}$. Consequently, in addition to a small Landau mixing, the condition to preserve the butterfly spectrum can be stated as

$$eaE \ll U_0 e^{-\pi\sigma/2}. \quad (50)$$

This condition restricts the intensity of both the electric and magnetic fields, these are estimated as (inserting units): $E \ll U_0/(ea) \sim 100 (U_0/\text{meV}) \text{ V/cm}$ and $B \geq \pi h/(ea^2) \sim 0.6T$.

Fig. 2 shows the energy spectrum for the four lowest Landau bands as a function of σ . In this case a higher coupling strength ($U_0 = 1.2 \text{ meV}$) yields important Landau mixing. For a strong magnetic field the electric field contribution is small and the spectrum is very similar to that previously obtained by Petschel and Geisel [30]. Three regimes can be identified in the plot: (i) In the strong magnetic field limit (small σ), the Landau bands are well separated and re-scaled butterfly structures are clearly observed. (ii) In the intermediate region ($\sigma \sim 1$) the periodic potential induces Landau level overlapping, (iii) as σ increase very narrow levels develop as a result of the electric field, this effect is clearly depicted in the right inset of Fig. 2.

The effects produced by the electric field can be clearly identified in Fig. 3 and Fig. 4, where the energy spectrum as a function of the electric field intensity ($\rho = eaE/U_0$) are displayed. In the first case (Fig. 3) Landau

mixing is neglected and the results for a single band and various selections of σ are displayed. We first notice that for $\sigma = 1/2$ and $\mathbf{E} = 0$ the two bands are degenerated at $\mathcal{E} = 0$, this degeneracy is lifted for $\sigma = 1.0038/2$; a further increment of σ to $\sigma = 1.1/2$ yields a transformation of the continuous bands into a series of quasi discrete levels. For $\sigma = 3/2$ the band structure is observed at small values of \mathbf{E} ; however as the electric field intensity is increased a transition from a continuous band to a discrete level spectrum is observed. The corresponding plot in Fig. 4 includes Landau mixing and shows the energy spectrum as a function of $(\rho = eaE/U_0)$ for the first two Landau bands. For $\sigma = 1/2$ every Landau level splits in two bands, the degeneracy is lifted by the finite Landau mixing. Again as E increases we observe that these bands evolve into a series of quasi discrete levels. In these plots we observe that the evolution from the band to discrete structure of the spectrum produces an interesting pattern in the distribution of gap regions, this structure can be related to a series of avoided and exact crossing effects of the quasienergies; these effects become more evident in Fig. 3c. It was pointed out in reference [31] that the coexistence of avoided and exact crossing of quasienergies in the Floquet spectrum can be understood on the basis of a generalized parity symmetry; in such a way that states belonging to the same parity number develop avoided crossing, but those of different parity symmetry can yield exact crossing.

In Fig. 5 the density of states as a function of the k_2 pseudomomentum and the quasienergy \mathcal{E} is displayed. The density of states was calculated from Green's function discontinuity obtained from the continued fraction expansion. Three values of $\sigma = 1/2, 3/2, 5/2$ are selected, consequently two bands appear when $\mathbf{E} = 0$. In the superior panels it is observed that both as E increases or B decreases, the spectrum for a fixed value of k_2 evolves into a set of narrow bands. When k_2 is varied the spectrum becomes almost continuous, except for the small gaps that open between the bands.

Based on the previous results it follows that the EMB model preserves the band structure. For weak electric fields the bands are grouped forming the “butterfly spectrum”; whereas as the intensity of \mathbf{E} increases the bands are replaced by a series of quasi discrete levels: a “magnetic Stark ladder”.

4.3 Adiabatic approximation

In this section we exhibit an alternative expression for the effective Schrödinger equation that governs the dynamics of the system. Based on this formalism

we shall find an approximated adiabatic solution, that throws further insight into the physical results obtained in the previous section. Let us consider the generalized Harper equation (48), taking into account that the matrix Q_m is periodic in m with period p , we find convenient to define the unitary transformation

$$d_l(\phi) = \sum_m \mathbb{U}_{l,m}(\phi) c_m, \quad \mathbb{U}_{l,m}(\phi) = \sqrt{\frac{qa}{2\pi}} e^{iqa\phi[m/p]} \delta_{l, m \bmod p}, \quad (51)$$

where $[m/p]$ denotes the integer part of the number, and the delta enforces the condition $l = m, \bmod p$. Notice that whereas the index m in c_m runs over all the integers, the corresponding label of the state $d_l(\phi)$ takes the values $l = 0, 1, 2, \dots, p-1$. The new vector state $d_l(\phi)$ satisfies the periodicity condition

$$d_l\left(\phi + \frac{2\pi}{qa}\right) = d_l(\phi), \quad (52)$$

and the transformation matrices fulfill the following properties

$$\begin{aligned} \sum_{m=-\infty}^{\infty} \mathbb{U}_{l,m}(\varphi) \mathbb{U}_{m,l'}^\dagger(\phi) &= \delta_{l,l'} \delta(\phi - \varphi), \\ \sum_{l=0}^{p-1} \int_0^{\frac{2\pi}{qa}} d\phi \mathbb{U}_{m,l}^\dagger(\phi) \mathbb{U}_{l,m'}(\phi) &= \delta_{m,m'}. \end{aligned} \quad (53)$$

Applying this transformation to the generalized Harper equation (48) yields

$$H_M(k_1 + \phi, k_2) d(k_1 + \phi, k_2) = \left(\mathcal{E} + Ek_2 - iE \frac{\partial}{\partial \phi} \right) d(k_1 + \phi, k_2), \quad (54)$$

where the Hamiltonian is reduced to a $p \times p$ block form

$$H_M(k_1 + \phi, k_2) = \begin{pmatrix} Q_0 & Q^+ & 0 & 0 & \dots & Q^- \\ Q^- & Q_1 & Q^+ & 0 & \dots & 0 \\ 0 & Q^- & Q_2 & Q^+ & \dots & 0 \\ \vdots & \vdots & \vdots & \vdots & \ddots & \vdots \\ Q^+ & 0 & 0 & 0 & \dots & Q_{p-1} \end{pmatrix} \quad (55)$$

here $Q^- \equiv Q^-(k_1 + \phi, k_2)$, $Q_m \equiv Q_m(k_1 + \phi, k_2)$ and $Q^+ \equiv Q^+(k_1 + \phi, k_2)$. Taking into account that each block in (55) is a $L \times L$ matrix determined by the Landau indexes, we have obtained that the transformation (51) reduces the infinite dimensional representation of the Schrödinger equation to a $pL \times pL$ representation. The price is that a non-local derivative term respect to parameter ϕ has been added. In the absence of electric field, Eq. (54) represents a finite dimensional eigenvalue problem, that can be solved by direct diagonalization. We observe from Eqs. (54) and (55) that ϕ appears to be directly related the longitudinal quasimomentum k_1 , in fact if we redefine $k_1 + \phi \rightarrow k_1$ in Eq. (54) yields

$$H_M(k_1, k_2) d(k_1, k_2) = \left(\mathcal{E} + Ek_2 - iE \frac{\partial}{\partial k_1} \right) d(k_1, k_2). \quad (56)$$

This expression confirms the form of the Schrödinger equation (30) previously discussed, in which the “dynamics” is determined by a differential equation with respect to the longitudinal quasimomentum. However we now have an explicit finite-dimensional matrix representation for the Hamiltonian.

Let the “instantaneous” eigenstates of H_M be $h^{(\alpha)}$ with energies $\Delta^{(\alpha)}$, i.e.

$$H_M h^{(\alpha)}(k_1, k_2) = \Delta^{(\alpha)}(k_1, k_2) h^{(\alpha)}(k_1, k_2), \quad (57)$$

where α labels the band state of the non-perturbed problem. A solution of Eq. (56) can readily be obtained in the adiabatic approximation as follows

$$d^{(\alpha)}(k_1, k_2) = \exp \left[-i \frac{\mathcal{E}}{E} k_1 + i \frac{1}{E} \int_0^{k_1} d\phi \Delta^{(\alpha)}(\phi, k_2) + i \gamma^{(\alpha)}(k_1, k_2) \right] h^{(\alpha)}(k_1, k_2), \quad (58)$$

where the Berry phase $\gamma(\phi)$ is determined from the substitution of the previous expression in Eq. (56)

$$\gamma^{(\alpha)}(k_1, k_2) = i \int_0^{k_1} d\phi h^{(\alpha)\dagger}(\phi, k_2) \frac{\partial}{\partial \phi} h^{(\alpha)}(\phi, k_2). \quad (59)$$

The energy eigenvalue is then determined by the periodicity condition (52), hence the change of the phase of the wave function (58) must be an integral

multiple of 2π , consequently the spectrum in the adiabatic approximation is given as

$$\mathcal{E}^{(\alpha)}(k_2) = nEa\sigma + \frac{qa}{2\pi} \int_0^{2\pi/qa} dk_1 \Delta^\alpha(k_1, k_2) + \frac{qaE}{2\pi} \gamma^{(\alpha)}(2\pi/qa, k_2), \quad n = 0, \pm 1, \dots \quad (60)$$

This result deserves some comments. The energy spectrum in the presence of electric and magnetic field contains a series of discrete levels separated by

$$\Delta\mathcal{E} = Ea\sigma = \frac{\hbar E}{aB}, \quad (61)$$

where we have used Eq. (11) and restored units. These levels are similar to the Wannier levels that appear when an electric field is applied to an electron in a periodic potential, the energy separation being proportional to aE . In the present case, the band structure parallel to the electric field is replaced by a set of discrete steps, this “magnetic Stark ladder” are characterized by a separation proportional to the electric field intensity, but inversely proportional to both the lattice separation and the magnetic field. The existence of these levels can be explained by the following argument. In the presence of simultaneous \mathbf{E} and \mathbf{B} fields, the electron travels between lattice points in a time $\tau = aB/E$. As long as the electron does not tunnel into another band, the motion appears as periodic, with frequency $\omega = 2\pi/\tau$, corresponding to a series of energy levels whose separation $\Delta\mathcal{E} = \hbar\omega$ coincides with the result in Eq. (61). This magnetic-Stark ladder is combined with the Hofstadter spectrum represented by the second term in Eq. (60) and the contribution of the Berry phase, the competition between these three factors was discussed in the numerical analysis of the previous section. We notice that the Berry phase is written as the integral of the longitudinal component of the Berry connection $\mathcal{A}_\alpha(\mathbf{k})$ discussed by Kohmoto [12].

5 Summary

We have considered the quantum mechanics of a periodic electron system driven by electric and magnetic fields. We presented a thorough discussion of the symmetries of the electric-magnetic Bloch problem. These symmetries were utilized in order to construct the wave function of the system.

The space-time representation of the wave function (33,34) fulfills the Bloch-Floquet theorem with modulation functions that satisfy the generalized Bloch conditions given in (35); the phases that appears in these conditions are determined by the dual-gauge potential related to the symmetry operators (7).

The dynamics of the system is governed by a finite difference equation (45), that represents a generalization of the Harper equation, the equation includes the following effects: (1) an arbitrary periodic potential, (2) an electric field orientated in a commensurable direction of the lattice, and (3) the coupling between different Landau levels. The model previously discussed by Petschel and Geisel [30], as well as the Harper equation (1) are recovered if the appropriated limit is enforced.

A detailed numerical analysis based on the solution via a matrix continued fractions was carried out, and the properties of the generalized Hofstadter spectrum were discussed. In the strong magnetic field limit the Landau bands are well separated and re-scaled butterfly structures emerge; in the intermediate region the periodic potential induces important Landau level overlapping; finally as the electric field intensity is increased a transition from a continuous band to a discrete level spectrum is observed. In this “magnetic Stark ladder” the equally spaced discrete levels are separated in integer multiple of $\hbar E/aB$. We find that in order to preserve the self-similarity structure of the Butterfly spectrum, besides the strong magnetic field condition $B \geq \pi\hbar/(ea^2)$, the electric field intensity should be restricted according to Eq. (50).

An effective equation of motion in k -space was derived (56). In this equation the “dynamics” is governed by a differential equation with respect to the longitudinal quasimomentum, the explicit matrix representation for the Hamiltonian is given in (55). Based on this formalism an approximated adiabatic solution for the energy spectrum (60) was obtained. This expression includes: (1) the discrete “magnetic Stark ladder” term (61), (2) and averaged Hofstadter contribution, and (3) the Berry phase contribution (59). This Berry phase is written as the integral of longitudinal component of the Berry connection discussed by Kohmoto [12] in relation with the quantization of the Hall conductance. We finally remark that the present formalism should set the basis for the study of the Hall conductivity beyond the linear response approximation.

We acknowledge the partial financial support endowed by CONACyT through grant No. *42026-F*.

References

- [1] R. Peierls, Z. Phys. 80 (1933) 763.
- [2] P. G. Harper, Proc. Phys. Soc. A 68 (1955) 874.
- [3] J. Zak, Phys. Rev. 134 (1964) A1602.
- [4] M. Y. Azbel', Sov. Phys. JETP 19 (1964) 634.
- [5] A. Rauh, Phys. Status Solidi B 69 (1975) K9.
- [6] I. Dana, J. Zak, Phys. Rev. B 28 (1982) B811.
- [7] P. G. Harper, J. Phys.: Condens. Matter 3 (1991) 3047.
- [8] J. Zak, Phys. Rev. Lett. 79 (1997) 533.
- [9] D. R. Hofstadter, Phys. Rev. B 14 (1976) 2239.
- [10] D. Thouless, M. Kohmoto, M. P. Nightingale, M. den Nijs, Phys. Rev. Lett. 49 (1982) 405.
- [11] Q. Niu, D. Thouless, Y.-S. Wu, Phys. Rev. B 31 (1985) 3372.
- [12] M. Kohmoto, Annals of Phys. 160 (1985) 343.
- [13] A. Kunold, M. Torres, Phys. Rev. B 61 (2000) 9879.
- [14] H. Nazareno, P. Brito, Phys. Rev B 64 (2001) 045112.
- [15] M. Torres, A. Kunold, Phys. Lett. A 323 (2004) 290.
- [16] A. Barelli, J. Bellissard, C. F, Phys. Rev.Lett. 83 (1999) 5082.
- [17] U. Kuhl, H. J. Stöckmann, Phys. Rev. Lett. 80 (1998) 3232.
- [18] O. Richoux, V. Pagneux, Europhys. Lett. 59 (2002) 34–20.
- [19] T. Schlösser, J. P. K. K. Ensslin, M. Holland, Europhys. Lett. 33 (1996) 683.
- [20] C. Albrecht, J. H. Smet, D. Weiss, K. von Klitzing, R. Hennig, M. Langenbuch, M. Suhrke, U. Rssler, V. Umansky, H. Schweizer, Phys. Rev. Lett. 83 (1999) 2234.

- [21] C. Albrecht, J. H. Smet, K. von Klitzing, D. Weiss, V. Umansky, H. Schweizer, Phys. Rev. Lett. 86 (2001) 147.
- [22] S. Aubry, C. Andre, Ann. Israel Phys. Soc . 3 (1980) 133.
- [23] N. Ashby, S. Miller, Phys. Rev. B 139 (1965) A428.
- [24] F. T. Hadjioannou, N. V. Sarlis, Phys. Rev. B 54 (1996) 5334.
- [25] F. T. Hadjioannou, N. V. Sarlis, Phys. Rev. B 56 (1997) 9406.
- [26] J. Zak, Phys. Rev. Lett. 71 (1993) 2623.
- [27] J. Zak, Phys. Rev. Lett. 19 (1967) 1385.
- [28] M. Moshinsky, C. Quesne, Journal of Mathematical Physics 12 (1971) 1772.
- [29] H. Risken, The Fokker-Planck Equation-Methods of Solution and Applications, Vol. 18 of Springer Series in Synergetics, Springer-Verlag, Berlin, 1984, Ch. 9.
- [30] G. Petschel, T. Geisel, Phys. Rev. Lett. 71 (1993) 239.
- [31] F. Grosmann, P. jung, T. Dittrich, P. Hanggi, Z. Phys. B 84 (1991) 315.

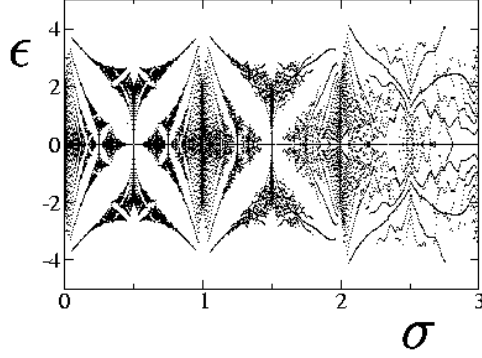


Figure 1: The energy spectrum inside the lowest Landau level as a function of the inverse magnetic flux σ . The energy axis is rescaled to $\epsilon = \mathcal{E} / [U_0 e^{-\pi\sigma/2}]$. All values of $k_1 \in [0, 2\pi/qb]$ are included. The parameters selected are: $m^* = 0.067m_e$, $a = 100 \text{ nm}$, $U_0 = 0.5 \text{ meV}$, $E = 0.5 \text{ V/cm}$, and $k_2 = \pi/2$.

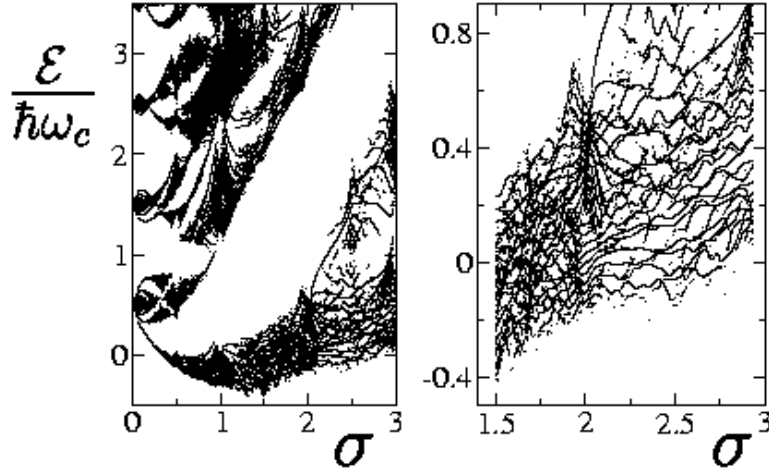


Figure 2: The energy spectrum for the four lowest Landau bands is plotted as a function of magnetic flux σ . The coupling strength $K = 6$ yields important Landau mixing. All values of $k_1 \in [0, 2\pi/qb]$ are included. The parameters selected are: $m^* = 0.067m_e$, $a = 100\text{ nm}$, $U_0 = 1.2\text{ meV}$, $E = 0.5\text{ V/cm}$, and $k_2 = \pi/2$. The right inset shows the details of the spectrum in a reduced region that was originated from the lowest Landau band. Seven Landau levels are included in the calculation in order to attain convergence.

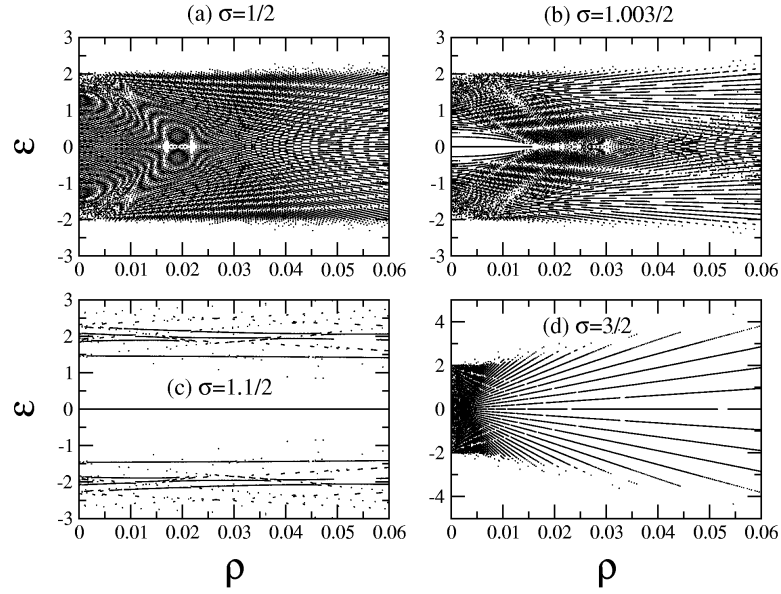


Figure 3: The energy spectrum for a single Landau level as a function of the electric field intensity ($\rho = eaE/U_0$) for: (a) $\sigma = \frac{1}{2}$, (b) $\sigma = \frac{1.0038}{2}$, (c) $\sigma = \frac{1.1}{2}$, (d) $\sigma = \frac{3}{2}$. The energy axis is rescaled to $\epsilon = \mathcal{E} / [U_0 e^{-\pi\sigma/2}]$. All values of $k_1 \in [0, 2\pi/qb]$ are included, and the other parameters are selected as: $m^* = 0.067m_e$, $a = 100 \text{ nm}$, $U_0 = 0.5 \text{ meV}$, and $k_2 = \pi/2$.

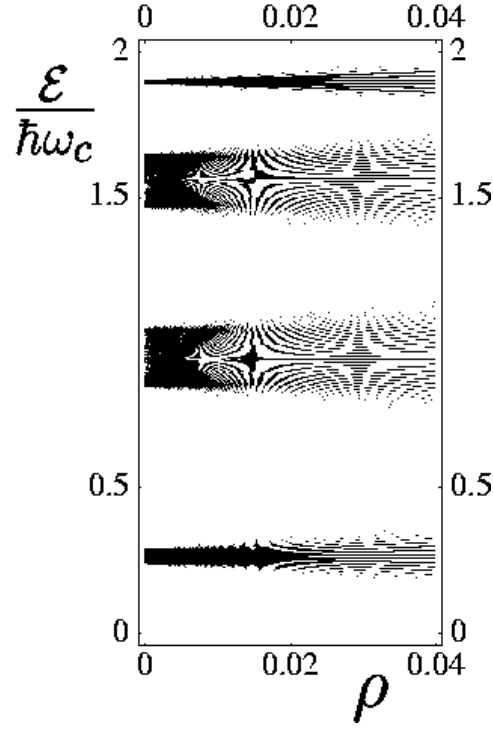


Figure 4: Energy density plot for the two lowest Landau levels as a function of the electric field intensity ($\rho = eaE/U_0$) for $\sigma = 1/2$. All values of $k_1 \in [0, 2\pi/qb]$ are included, the other parameters take the same values as in Fig. 2.

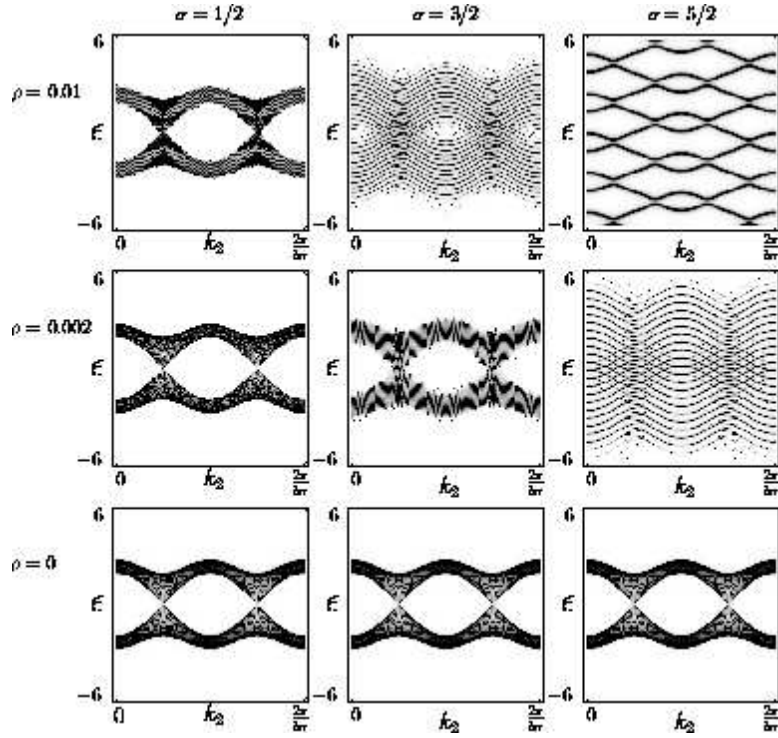


Figure 5: Energy density plot for the lowest Landau levels as a function of the transversal pseudomomentum k_2 . Three values of $\sigma = 1/2, 3/2, 5/2$ are selected, so two bands appear when $E = 0$. Three values of E are considered: $\rho = eaE/U_0 = 0, 0.002, 0.01$.